Hybrid Stiff/Compliant Workspace Control for Robotized Minimally Invasive Surgery

Pål Johan From, Jang Ho Cho, Anders Robertsson, Tomohiro Nakano, Mahdi Ghazaei, and Rolf Johansson

Abstract— This paper presents a novel control architecture for hybrid stiff and compliant control for minimally invasive surgery which satisfies the constraints of zero lateral velocity at the entry point for serial manipulators. For minimally invasive surgery it is required that there is no sideways motion at the point where the robots enter the abdomen. This is necessary to avoid any damage to the patient's body when the robot moves. We solve this at a kinematic level, i.e., we find a Jacobian matrix that maps the velocities in joint space to the end-effector velocities and at the same time guarantees that certain velocities at the entry point are zero. Because the new velocity variables are defined in the end-effector workspace we can use these for hybrid motion/force control. The approach is verified experimentally by implementing hybrid stiff and compliant control of the end effector and we show that the insertion point constraints are always satisfied.

I. Introduction

Minimally invasive telesurgical systems allow for surgical procedures to be performed with less patient trauma and risk, in addition to shorter patient recovery times. This is achieved by inserting the surgical instruments into the body through small insertion points called trocars, often together with a camera for visual feedback. Such systems thus provide a safe environment for surgeons to perform telesurgery, either in-house or remotely through a communication channel [1]. Robot-assisted telesurgical systems also allow for more dexterous surgical procedures than classic laparoscopic surgery in addition to enhanced overall performance, for example by scaling and filtering out hand tremor [2].

When inserting the robotic tool into the patient it is crucial to avoid any lateral motion. This can be obtained in one of three ways: i) The remote center of motion (RCM) can be obtained mechanically by using a parallel device that keeps the RCM fixed, such as in the DaVinci robot from Inuitive Surgical [1]. This is a safe solution, but not flexible when it comes to changing the RCM during operation. ii) The RCM can also be implemented using two passive joints that form a universal joint together with four active joints that generates the desired 4-DoF motion. iii) Finally a software-based RCM can be implemented by controlling the robot so

that the lateral motion at the trocar is eliminated. This is the approach discussed in this paper.

Because the surgical instruments are located very close to the patient's internal organs, tissues, and bones, a compliant behavior at the end effector is desirable to avoid inflicting damage on the patient. On the other hand, if the surgeon is to perform interaction tasks such as cutting and suturing, a compliant behavior is not appropriate, at least for some directions of the end-effector workspace. For cutting procedures, for example, the surgeon should be able to move the knife in the cutting direction and also apply forces in this direction. In other directions such as the directions orthogonal to the motion, one might opt for a guided motion and compliant behavior in order to keep the surgeon on the right trajectory, or to protect other internal organs. These requirements call for a hybrid control with stiff motion control in some directions of the end-effector workspace and compliant behavior in other directions. Such a control scheme is only possible when the state space is written in terms of the end-effector variables, which is not straight forward when constraints are present in the kinematic chain.

Hybrid control in the end-effector space has been studied in detail by many authors [3]. Mason [4] introduced natural constraints—which correspond to the degrees of freedom where the environment imposes position or force constraints on the end-effector motion— and artificial constraint—which are the constraints imposed by the controller. Because the natural constraints are orthogonal to the artificial constraints, the end-effector space can be divided into two subspaces where only the latter can be controlled. For an appropriate choice of reference frame, selection matrices can be defined for hybrid position/force control [5], [6], [7]. A similar but more geometric approach was presented in Lipkin and Duffy [8] where the concept of reciprocity is used to define the two subspaces.

In the setting of minimally invasive surgery Deal and Newman [9], [10] present a method for stiff control at the entry point and compliant control at the end effector. A combination of hybrid force/position control and Natural Admittance Control (NAC) is used to satisfy the portal constraints and at the same time allows for compliant behavior at the end-effector. The resulting controller divides the control efforts into a 2-DoF stiff control at the entry point and a 4-DoF NAC controller at the end effector. The approach thus allows for a stiff entry point and a compliant behavior at the end effector. The approach can not, however, be directly extended to also allow for hybrid control of the 6-DoF end-effector motion, as all the degrees of freedom at the end-

effector will have a compliant behavior. In this paper we propose a novel approach which in addition to satisfy the entry point constraints also allows for hybrid control of the end-effector, i.e., some directions can take on a compliant behavior while others are stiff/position controlled.

The constraints imposed by the entry point are often referred to as the Remote Center of Motion (RCM). Several researchers have addressed the problem of imposing the RCM constraints on the robot motion by modifying the controller. Early results solved the motion constraints as an optimization problem, for example in Funda et al. [11] and Li et al. [12]. In Ortmaier and Hirzinger [13] the RCM kinematics is derived and used to estimate the position of the entry point for a robot with passive joints. The passive joints guarantee that no forces are exerted to the entry point. In Locke and Patel [14] the kinematic model is used to derive an optimization technique that allows isotropy of the surgical tool to be evaluated subject to the RCM constraint. Trocar kinematics is also discussed in Lenarčič and Galletti [15].

Azimian et al. [16] uses the concept of task priority and restricted Jacobian to derive the constrained motion in terms of the trocar and manipulator geometry. The end-effector motion is found in the standard way from the manipulator Jacobian, which is taken from the null space of the constraint Jacobian of the entry point. The constraint Jacobian is found in the normal way by the mapping from the joint space velocities to the lateral linear velocities of the RCM point. The constraints at the insertion point are given first priority and the end-effector motion is given a secondary priority as this is taken from the null space of the first Jacobian [17]. The approach depends on the kinematics of both the robotic manipulator and the trocar.

In this paper we take a somewhat different approach in that we impose the constraints on the velocity twist of the last link of the robot directly and rewrite the mapping from the end-effector twists to the joint velocities so that it is guaranteed to satisfy the RCM constraints. The main advantage of the proposed approach is that the constrained system can be treated in the same way as a standard unconstrained manipulator simply by replacing the standard Jacobian with the constrained Jacobian, and we can therefore apply any conventional control scheme used for unconstrained robots. In other words, when it comes to control there is no difference between constrained and unconstrained robotic manipulators, except for the Jacobian. We can for example formulate the control problem in the end-effector space using standard control laws, including hybrid control, and map these to the joint velocities, which are effectuated in the normal way by the low-level robot controller. We thus obtain a formulation that is independent of the robot kinematics and allows for simple implementation as we can use existing low-level controllers both for the robot and the end-effector.

II. System Overview and Problem Formulation

The system discussed in this paper consists of a standard or customized 6-DoF robotic manipulator with a shaft, i.e., a thin long link used for inserting the end effector into the body
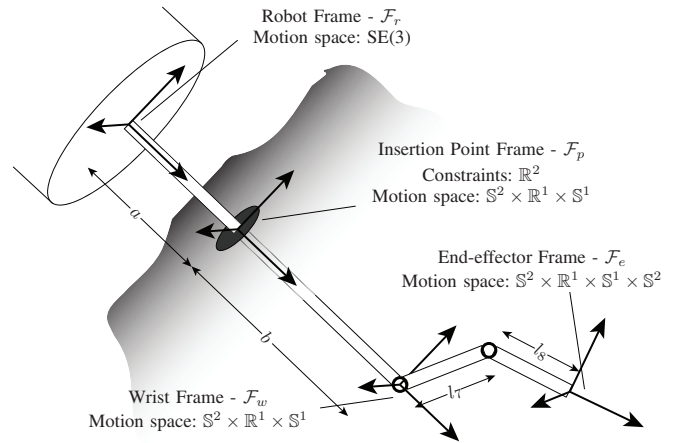

Fig. 1. The robotic setup discussed in this paper. The shaft is inserted into the body through a trocar at $\mathcal{F}_p$. The motion spaces of the different frames are subgroups of $SE(3)$ defined by linear motion $\mathbb{R}$, circular motion $\mathbb{S}$, and the sphere $\mathbb{S}^2$.

through the trocar. At the end of the shaft there is a wrist with two or more additional degrees of freedom and a tool. At the insertion point we will require that the sideways velocities are eliminated to prevent the robot from damaging the patient's tissue. This requirement imposes a 2-DoF constraint on the shaft so that the end of the shaft has 4 DoF of motion. The additional degrees of freedom in the wrist give the end effector a full 6-DoF motion. Most endoscopic wrists, such as the one used in the Intuitive Surgical's da Vinci robots, have 3 degrees of freedom. This paper is not concerned with redundancy, so we consider the case where the wrist has 2 DoF. The system setup and the configuration spaces used in this paper are shown in Fig. 1.

The problem considered consists of maintaining a stiff control of zero velocity at the insertion point while allowing for a combination of stiff and compliant control at the end effector. Several surgical tasks require both position and force control in the different directions of the end-effector coordinate frame. Other tasks do not require the specifications of all the 6 DoF of the configuration space so the remaining directions are often given a compliant behavior to prevent the tool from damaging tissues or organs. This requires a well defined workspace representation that can be used to divide the workspace into suitable orthogonal or reciprocal spaces.

In this paper we propose a new approach where the insertion point constraints are taken care of at a kinematic level and satisfied by defining a constrained Jacobian matrix that guarantees that the constraints are satisfied, independently of the commanded master reference. The Jacobian gives the mapping from the joint space to the end-effector space on which hybrid position/force control can be applied in the normal way.

III. Constrained Kinematics

In this section we derive the kinematics of the robotic system when the kinematic constraints at the entry point are satisfied.

A. End-effector Motions

We will attach a frame $\mathcal{F}_r$ to the last link of the 6-DoF robotic manipulator, as illustrated in Fig. 1. The body velocities of this frame with respect to a fixed inertial frame $\mathcal{F}_0$ is represented by

$$V_{0r}^B = \begin{bmatrix} v_x^r & v_y^r & v_z^r & \omega_x^r & \omega_y^r & \omega_z^r \end{bmatrix}^\mathsf{T}. \qquad (1)$$

The robot velocities can be found from the joint velocities by the Jacobian in the standard way as $V_{0r}^B = J_r^B(q_r)\dot{q}_r$ where $J_r^B(q_r)$ is the geometric Jacobian relating the joint velocities and the body twist of the last link of the robot.

One of the control objectives is to maintain zero translational velocity at the entry point. We will thus also define a reference frame $\mathcal{F}_p$ at this point with body velocity twist

$$V_{0p}^B = \begin{bmatrix} v_x^p & v_y^p & v_z^p & \omega_x^p & \omega_y^p & \omega_z^p \end{bmatrix}^\mathsf{T}. \qquad (2)$$

The reference frames are illustrated in Fig. 1. The relation between the velocity at the last link of the robot and the entry point, i.e., the point $p_{rp} = \begin{bmatrix} 0 & 0 & a \end{bmatrix}^\mathsf{T}$ in frame $\mathcal{F}_r$, is given by the simple relation

$$\begin{aligned}
\begin{bmatrix} v_x^p \\ v_y^p \\ v_z^p \end{bmatrix} &= \begin{bmatrix} v_x^r \\ v_y^r \\ v_z^r \end{bmatrix} + \begin{bmatrix} \omega_x^r \\ \omega_y^r \\ \omega_z^r \end{bmatrix} \times \begin{bmatrix} 0 \\ 0 \\ a \end{bmatrix} \\
&= \begin{bmatrix} v_x^r + a\omega_y^r \\ v_y^r - a\omega_x^r \\ v_z^r \end{bmatrix}
\end{aligned} \qquad (3)$$

while the angular velocities are identical: $\omega_{0p}^B = \omega_{0r}^B$.

If we assume that the requirement of zero velocity at the insertion point is satisfied, for example by a simple position control law or a physical constraint, we see from Equation (3) and the properties of rigid bodies that the velocity at this point can be written in terms of the velocities at $\mathcal{F}_r$ as

$$V_{0p}^B = \begin{bmatrix} 0 & 0 & v_z^r & \omega_x^r & \omega_y^r & \omega_z^r \end{bmatrix}^\mathsf{T}. \qquad (4)$$

At the end of the shaft we attach the wrist frame $\mathcal{F}_w$. The wrist frame has only four degrees of freedom and can thus be written in terms of the velocities at the last robot link (or alternatively the entry point) as

$$V_{0w}^B = \begin{bmatrix} v_x^w \\ v_y^w \\ v_z^w \\ \omega_x^w \\ \omega_y^w \\ \omega_z^w \end{bmatrix} = \begin{bmatrix} 0 & 0 & b & 0 \\ 0 & -b & 0 & 0 \\ 1 & 0 & 0 & 0 \\ 0 & 1 & 0 & 0 \\ 0 & 0 & 1 & 0 \\ 0 & 0 & 0 & 1 \end{bmatrix} \begin{bmatrix} v_z^r \\ \omega_x^r \\ \omega_y^r \\ \omega_z^r \end{bmatrix}. \qquad (5)$$

Finally the velocity of the end-effector frame $\mathcal{F}_e$ is found by adding the velocity of the wrist frame with respect to the inertial frame to the velocity of the end effector with respect to the wrist frame [18]:

$$V_{0e}^B = \mathrm{Ad}_{g_{ew}} V_{0w}^B + V_{we}^B. \qquad (6)$$

To simplify the expressions we assume that the last two joints rotate about the x-axis and we set $l_8 = 0$. The body velocity at the end effector then becomes [19]

$$V_{0e}^B = \begin{bmatrix} b\omega_y^r + l_7\cos q_7\omega_y^r + l_7\sin q_7\omega_z^r \\ \sin q_{78}v_z^r - (b\cos q_{78} + l_7\cos q_8)\omega_x^r - l_7\cos q_8\dot{q}_7 \\ \cos q_{78}v_z^r + (b\sin q_{78} + l_7\sin q_8)\omega_x^r + l_7\sin q_8\dot{q}_7 \\ \omega_x^r + \dot{q}_7 + \dot{q}_8 \\ \cos q_{78}\omega_y^r + \sin q_{78}\omega_z^r \\ -\sin q_{78}\omega_y^r + \cos q_{78}\omega_z^r \end{bmatrix} \qquad (7)$$

where we have used that $R_{ew} = R_{er}$ and $q_{78} = q_7 + q_8$. For most telesurgical systems the wrist is close to a spherical joint so we can assume that $l_7, l_8 << b$ and we get

$$V_{0e}^B \approx \begin{bmatrix} b\omega_y^r \\ \sin q_{78}v_z^r - b\cos q_{78}\omega_x^r \\ \cos q_{78}v_z^r + b\sin q_{78}\omega_x^r \\ \omega_x^r + \dot{q}_7 + \dot{q}_8 \\ \cos q_{78}\omega_y^r + \sin q_{78}\omega_z^r \\ -\sin q_{78}\omega_y^r + \cos q_{78}\omega_z^r \end{bmatrix}. \qquad (8)$$

B. Constrained Jacobian Matrix

With the formulation above we have assumed that the lateral velocity at the entry hole is zero. To guarantee this, we need a design that satisfies this requirement and these variables therefore need to be included in the state space representation. The state space can then be written as a vector in $\mathbb{R}^8$:

$$v^p = \begin{bmatrix} v_x^p & v_y^p & v_z^p & \omega_x^p & \omega_y^p & \omega_z^p & \dot{q}_7 & \dot{q}_8 \end{bmatrix}^\mathsf{T}. \qquad (9)$$

This choice of state variables is very useful when controlling the velocity at the entry point (the two first variables) to zero. It is also convenient because it can be found directly from the robot kinematics (first 6 variables) and the end-effector kinematics (last 2 variables), i.e.,

$$v^r = \begin{bmatrix} v_x^r & v_y^r & v_z^r & \omega_x^r & \omega_y^r & \omega_z^r & \dot{q}_7 & \dot{q}_8 \end{bmatrix}^\mathsf{T} \qquad (10)$$

and we can find Equation (9) directly from Equation (3).

On the other hand, the end-effector velocities written in this way are not particularly useful because these are not the velocities that we want to control. A more appropriate choice of state variables for our problem is therefore found as

$$v^e = \begin{bmatrix} v_p^p \\ V_{0e}^B \end{bmatrix} = \begin{bmatrix} v_x^p & v_y^p & v_x^e & v_y^e & v_z^e & \omega_x^e & \omega_y^e & \omega_z^e \end{bmatrix}^\mathsf{T}. \qquad (11)$$

This representation of the velocity vector is suitable for both stiff control at the entry point and hybrid control of the end effector. The velocity vector v^e relates to the velocities v^r by

$$v^e = J_{er}v^r. \qquad (12)$$

Note that this is a mapping from one representation using body velocities to another representation also in body velocities. The coordinate transformation matrix J_{er} can be found as in (13).

$$
\begin{bmatrix} v_x^p \\ v_y^p \\ v_x^e \\ v_y^e \\ v_z^e \\ \omega_x^e \\ \omega_y^e \\ \omega_z^e \end{bmatrix} =
\begin{bmatrix}
1 & 0 & 0 & 0 & a & 0 & 0 & 0 \\
0 & 1 & 0 & -a & 0 & 0 & 0 & 0 \\
1 & 0 & 0 & 0 & (a+b)+l_7\cos q_7 & l_7\sin q_7 & 0 & 0 \\
0 & \cos q_{78} & \sin q_{78} & -(a+b)\cos q_{78}-l_7\cos q_8 & 0 & 0 & -l_7\cos q_8 & 0 \\
0 & -\sin q_{78} & \cos q_{78} & (a+b)\sin q_{78}+l_7\sin q_8 & 0 & 0 & l_7\sin q_8 & 0 \\
0 & 0 & 0 & 1 & 0 & 0 & 1 & 1 \\
0 & 0 & 0 & 0 & \cos q_{78} & \sin q_{78} & 0 & 0 \\
0 & 0 & 0 & 0 & -\sin q_{78} & \cos q_{78} & 0 & 0
\end{bmatrix}
\begin{bmatrix} v_x^r \\ v_y^r \\ v_z^r \\ \omega_x^r \\ \omega_y^r \\ \omega_z^r \\ \dot q_7 \\ \dot q_8 \end{bmatrix} \tag{13}
$$

The mapping between the workspace velocities and the joint velocities are found by the geometric Jacobian J_r^B:

$$
\begin{aligned}
\begin{bmatrix} v_p^p \\ V_{0e}^B \end{bmatrix} &= \begin{bmatrix} J_{er,a} & 0_{2\times 2} \\ J_{er,1} & J_{er,2} \end{bmatrix} \begin{bmatrix} V_{0p}^B \\ \dot q_w \end{bmatrix} \\
&= \begin{bmatrix} J_{er,a} & 0_{2\times 2} \\ J_{er,1} & J_{er,2} \end{bmatrix} \begin{bmatrix} J_r^B & 0 \\ 0 & I \end{bmatrix} \begin{bmatrix} \dot q_r \\ \dot q_w \end{bmatrix} \\
&= \begin{bmatrix} J_{er,a} J_r^B & 0_{2\times 2} \\ J_{er,1} J_r^B & J_{er,2} \end{bmatrix} \begin{bmatrix} \dot q_r \\ \dot q_w \end{bmatrix}.
\end{aligned} \tag{14}
$$

We will denote this matrix J_{eq} and write

$$
v^e = J_{eq}\dot q. \tag{15}
$$

C. Minimal Representation with Insertion Point Constraints

From (13) we see that the velocities at the entry point can be written in terms of the robot velocities as

$$
v_x^p = v_x^r + a\omega_y^r \tag{16}
$$
$$
v_y^p = v_y^r - a\omega_x^r \tag{17}
$$

and the constraint of zero velocity can therefore be cast into the following simple form

$$
v_x^r = -a\omega_y^r \tag{18}
$$
$$
v_y^r = a\omega_x^r \tag{19}
$$

where we need to know the distance from the last link of the robot to the entry point. We can incorporate these constraints in the kinematics (13) by introducing new variables v_1 and v_2 such that

$$
v_x^r = v_1 \qquad\qquad \omega_y^r = -\frac{1}{a}v_1 \tag{20}
$$
$$
v_y^r = v_2 \qquad\qquad \omega_x^r = \frac{1}{a}v_2. \tag{21}
$$

Substituting this into (13) and eliminating the entry point velocities that are now known to be zero gives Equation (22). This is suitable for workspace control and at the same time guarantees that the entry point velocity constraints are satisfied. In the controller v_1 and v_2 are realized through the expressions found in Equations (20) and (21). We will denote the matrix in Equation (22) that gives us the minimum representation of the end-effector workspace as J_{er}^m and this important transformation as $V_{0e}^B = J_{er}^m v_m^r$.
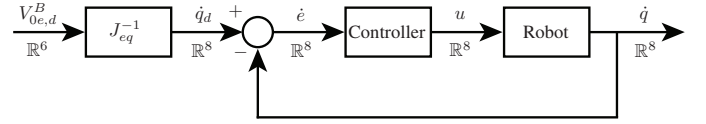
Fig. 2. One example of how the Constraint Jacobian J_{eq} can be used to obtain both control objectives. Note that the controller can be implemented at joint level in the normal way.

IV. HYBRID STIFF AND COMPLIANT CONTROL SCHEMES

In the previous section we found a state space representation well suited for implementing a hybrid control scheme in the end-effector space. We obtained this by the one-to-one mapping in (22) which gives the constraint robot motion from the desired end-effector motion by imposing the entry-point constraints. In this section we will study different approaches that can be used to obtain the required characteristics at the end-effector for which the entry-point constraints are satisfied. Common for all the formulations is that we define the task specifications in the new workspace variables, and use the transformations derived in the previous section to obtain the corresponding joint motions.

Our objective is to allow for both compliant and stiff control when the end-effector is in contact with the environment. At the same time stiff control is required at the entry point, which is solved at a kinematic level, i.e., through the Constraint Jacobian. Following the seminal work of Mason [4] and Craig and Raibert [5] we will define orthogonal workspaces for position and force control of the end effector. Mason [4] represented physical constraints by zero velocity and zero force in certain directions of the end-effector workspace and denoted these as natural constraints. Then the artificial constraints, or control, were defined subject to a certain control objective so that the natural constraints were always satisfied. The physical and artificial constraints are represented in terms of selection matrices S_p and S_f where, for a suitable choice of state space, we can choose S_p as a diagonal matrix representing the directions with free motion, and thus force cannot be applied, and S_f as representing the directions with constrained motion, which allow for force control.

A. Position Control

We will first look at a simple position control, i.e., we want the end effector to follow a master manipulator, in addition to satisfying the constraints at the insertion point. Stiff control

$$\begin{bmatrix} v_x^e \\ v_y^e \\ v_z^e \\ \omega_x^e \\ \omega_y^e \\ \omega_z^e \end{bmatrix} = \begin{bmatrix} -\frac{1}{a}(b + l_7 \cos q_7) & 0 & 0 & l_7 \sin q_7 & 0 & 0 \\ 0 & -\frac{1}{a}(b \cos q_{78} + l_7 \cos q_8) & \sin q_{78} & 0 & -l_7 \cos q_8 & 0 \\ 0 & \frac{1}{a}(b \sin q_{78} + l_7 \sin q_8) & \cos q_{78} & 0 & l_7 \sin q_8 & 0 \\ 0 & \frac{1}{a} & 0 & 0 & 1 & 1 \\ -\frac{1}{a} \cos q_{78} & 0 & 0 & \sin q_{78} & 0 & 0 \\ \frac{1}{a} \sin q_{78} & 0 & 0 & \cos q_{78} & 0 & 0 \end{bmatrix} \begin{bmatrix} v_1 \\ v_2 \\ v_z^r \\ \omega_z^r \\ \dot{q}_7 \\ \dot{q}_8 \end{bmatrix}. \qquad (22)$$

of this kind is necessary in many applications where the end effector is to follow a reference path as closely as possible. The approach described here will also serve as a benchmark for the approach presented in the next section. With this approach we do not want to control the interaction forces, but rather force the end-effector to follow the position dictated by the operator. If natural constraints are present, this will be communicated to the operator through force feedback. Position control thus fits into the framework described above by choosing $S_p = I$ and $S_f = 0$.

The control law can also be derived in joint space as shown in Fig. 2. First write the manipulator dynamics as

$$M_q(q)\ddot{q} + C_q(q, \dot{q})\dot{q} = \tau. \qquad (23)$$

Here M_q is the robot inertia matrix, $C_q(q, \dot{q})$ represent the Coriolis and centripetal forces, τ is the joint torques, and

$$M_q(q) = J_{eq}^{-\mathsf{T}} M J_{eq}^{-1}$$
$$C_q(q, \dot{q}) = J_{eq}^{-\mathsf{T}} \left(C - M J_{eq}^{-1} \dot{J}_{eq} \right) J_{eq}^{-1}$$

where M and C represent the dynamics in v^e. In this case we use the Jacobian that we found in (15) to obtain the dynamics in joint variables.

An inverse dynamics control law is then given by

$$\tau = M_q(q)y \qquad (24)$$

where we choose y as

$$y = \ddot{q}_d + K_D(\dot{q}_d - \dot{q}) + K_P(q_d - q) \qquad (25)$$

which guarantees that the error converges to zero [20]. Note that this control law is a kind of computed-torque control method. We see that the Constraint Jacobian J_{eq} allows us to reformulate the control problem into a standard control law in joint variables which guarantees that the insertion point constraints are satisfied (solved at a kinematic level) and that the master reference is followed (solved by the controller (24-25)).

A joint-space impedance control can also appear in the wrist control with a modification of Eqs. (24-25). Introduce the control law

$$\tau = M_q(q)y + J_F^T F - M_q(q)F \qquad (26)$$

where J_F^T is the Jacobian with respect to the force-sensing position. In addition to the computed-torque term, there is one force-compensating term and one term that provides impedance control with a computed-torque-like impedance dynamics in joint space:

$$M_q(q)(\ddot{\tilde{q}} + K_D\dot{\tilde{q}} + K_P\tilde{q} - F) = 0. \qquad (27)$$

Passivity can be shown for the mapping from F to $\dot{\tilde{q}}$ where $\tilde{q} = q_d - q$.

B. Impedance Control with Insertion Point Constraints

Impedance control for minimally invasive surgery is challenging because the impedance control needs to be implemented in the end-effector space while the constraints on the robot motion needs to be so that the velocities at the insertion point are zero. One solution to this problem is shown in Fig. 3. The desired motion is given by the master velocities $V_{0e,d}^B$. For impedance control we define a compliant frame $\mathcal{F}_c$ which gives the position and orientation of the end effector when it is in contact with the environment, i.e., the deviation from the desired frame $\mathcal{F}_d$ due to the sensed end-effector forces [3]. When the end effector is in contact with the environment it will thus follow the frame $\mathcal{F}_c$ which relates to the desired trajectory frame $\mathcal{F}_d$ by

$$M_c\ddot{p}_{dc} + D_c\dot{p}_{dc} + K_cp_{dc} = F_e \qquad (28)$$

which gives a new desired motion represented by the frame $\mathcal{F}_c$ whenever the robot is in contact with the environment.

We also need to guarantee that the velocities at the insertion point are zero. This is guaranteed by introducing the variables v_1 and v_2 as in Equation (22). The matrix $(J_{er}^m)^{-1}$ thus gives us the motion of the manipulator arm for which the constraints are satisfied. This is given by the four degrees of freedom velocity vector $v^r = \begin{bmatrix} v_1 & v_2 & v_x^r & \omega_z^r \end{bmatrix}^{\mathsf{T}}$. The six degrees of freedom motion of the manipulator arm is thus found by

$$\begin{bmatrix} v_x^r \\ v_y^r \\ v_z^r \\ \omega_x^r \\ \omega_y^r \\ \omega_z^r \end{bmatrix} = \begin{bmatrix} 1 & 0 & 0 & 0 \\ 0 & 1 & 0 & 0 \\ 0 & 0 & 1 & 0 \\ 0 & \frac{1}{a} & 0 & 0 \\ -\frac{1}{a} & 0 & 0 & 0 \\ 0 & 0 & 0 & 1 \end{bmatrix} \begin{bmatrix} v_1 \\ v_2 \\ v_z^r \\ \omega_z^r \end{bmatrix}. \qquad (29)$$

We now give this as input to the robot arm, together with the wrist motion, also found by the inverse of (22), and we separate the feedback loops for the manipulator arm and the wrist, as shown in Fig. 3.

We note that we have obtained compliant control in the end-effector workspace and we also guarantee that the insertion point constraints are satisfied, as required. If hybrid control is desired, we introduce selection matrices S_p and S_f in the normal way in the hybrid impedance controller in Fig. 3. Note also that we only use the velocity variables in the controller. This is not a problem in teleoperation, as the position variables are normally compensated for by the
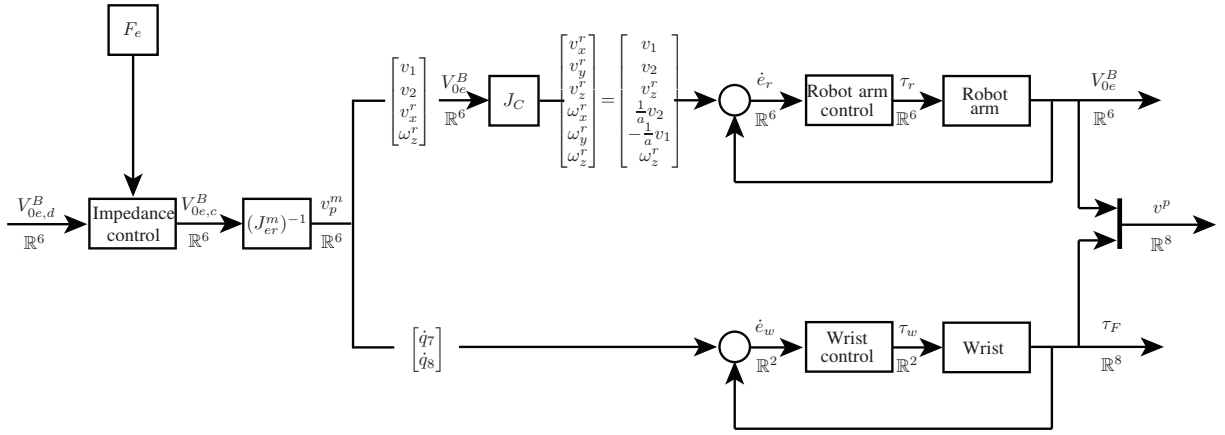
Fig. 3. Hybrid control scheme with insertion point constraints taken care of at a kinematic level.

operator, and we are mainly interested in following the velocity reference. In the impedance controller, however, we need both the acceleration and position variables. We therefore need to include a memory in the impedance controller so that the position can be recovered whenever spring forces are required.

V. EXPERIMENTS

In this section, the proposed control scheme is tested experimentally. To evaluate the applicability of the proposed method to robotic telesurgery, a teleoperation system is implemeted. For simplicity, we consider the wrist as the end effector which means the wrist does not have any DoF.

A. Experimental Set-up

The experimental set-up consists of a master device and a slave robot. The Omega 7 haptic device from Force Dimension which is a parallel haptic device is used as the master device. An ABB IRB140 industrial robot with a force/torque sensor at the tip, the 100M40 from JR3, is used as the slave robot.

The proposed control scheme is implemented by MAT-LAB Simulink and Real-Time Workshop. Input and output signals are received and sent through Ethernet from/to master and slave devices. The controller takes velocities and positions of the master device and force signals of the slave robot as inputs and generates desired joint velocities of the slave robot as output signals. The slave robot is controlled by its internal controller to follow the desired motions of each joint, details can be found in [21].

B. Experimental Results

Several experiments were performed including a stiff position control and an impedance control. In Fig. 4, an image is created by overlaying the motions of the slave robot during the experiments. The insertion point is virtually imposed in the middle of end effector and it can be recognized in Fig. 4. For clear illustration of the velocity constraints on the insertion point, we draw the traces of the end-effector of the experiment in Fig. 5. The color of the end-effector changes from gray to grayish red-violet with time. It is clearly shown
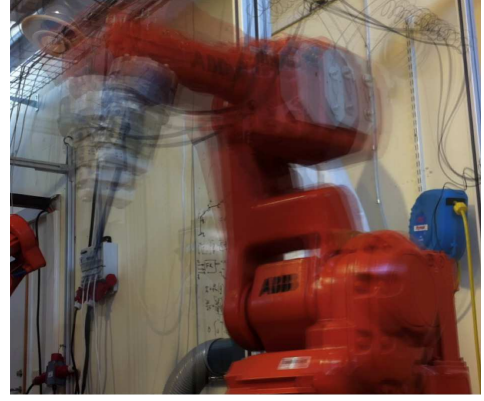

Fig. 4. Image overlay of the slave robot during the experiment.

that the proposed control scheme satisfies the zero-velocity constraints on the virtual insertion point. When noise is removed, the lateral motions that we measure at this point is zero, as expected.

We have also conducted experiments with impedance control. For clear illustration of the impedance control, the impedance controller is implemented along with the insertion direction which is the z-axis in robot frame and the inputs of the control scheme, $V_{0e,d}^B$, are also transformed to robot frame $\mathcal{F}_r$. To see the compliance along the z-axis, positions of the master device and the slave robot are drawn in Fig. 6. The contact along the z-axis has a duration of about $29s$. As a result of the impedance control, we see that the desired velocities of the slave robot are modified, as expected. It is noteworthy that the impedance controller is implemented in priori to the kinematic constraints as described in Fig. 3 which enables us to restrict the velocities at the insertion point.

VI. CONCLUSION

In this paper, we propose a novel control architecture for hybrid stiff and compliant control for minimally invasive surgery which satisfies the constraints of zero lateral velocity at the entry point. These constraints are handled on a
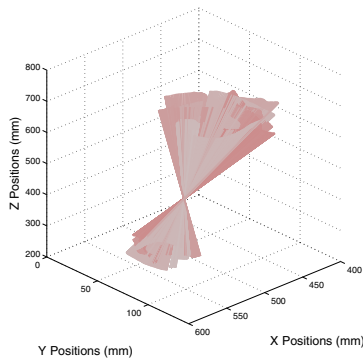
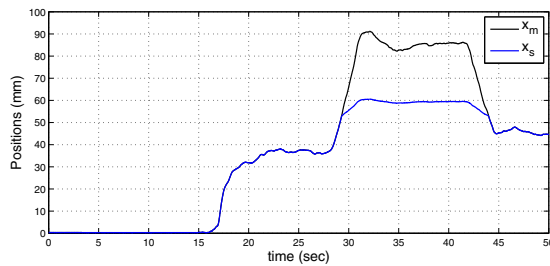Fig. 5.   Traces of the end effector during the experiment, illustrated in Cartesian space coordinate.

Fig. 6.   Z-axis positions of the master device and the slave robot in robot frame $\mathcal{F}_r$. Note that compliant motions are allowed through the proposed control scheme.

kinematic level by a Jacobian matrix that maps the velocities in joint space to the end-effector velocities and at the same time guarantees that the velocities at the entry point are zero. Both stiff position control and hybrid stiff/compliant control can be easily implemented in the end-effector workspace. The proposed approach is verified through experimental verification via stiff position control and hybrid control and we show that the insertion point constraints are satisfied in both cases.

REFERENCES

[1] G. Guthart and J. Salisbury Jr, "The intuitive^{TM} telesurgery system: overview and application," in *Proc. IEEE Int. Conf. Rob. Aut.*, pp. 618–621, 2000.

[2] D. Nio, R. Balm, S. Maartense, M. Guijt, and W. Bemelman, "The efficacy of robot-assisted versus conventional laparoscopic vascular anastomoses in an experimental model," *Eur. J. Vasc. Endovasc.*, vol. 27, no. 3, pp. 283–286, 2004.

[3] C. Natale, *Interaction Control of Robot Manipulators: Six-degrees-of-freedom Tasks*. Springer Tracts in Advanced Robotics, Springer, 2003.

[4] M. T. Mason, "Compliance and force control for computer controlled manipulators," *IEEE Trans. Systems, Man and Cybernetics*, vol. 11, pp. 418 –432, june 1981.

[5] J. Craig and M. Raibert, "A systematic method of hybrid position/force control of a manipulator," in *Proc. Computer Software and Applications Conference,*, pp. 446 – 451, 1979.

[6] A. Abbati-Marescotti, C. Bonivento, and C. Melchiorri, "On the invariance of the hybrid position/force control," *Journal of Intelligent and Robotic Systems*, vol. 3, no. 4, pp. 233–250, 1990.

[7] H. Bruyninckx and J. De Schutter, "Specification of force-controlled actions in the "task frame formalism"-a synthesis," *IEEE Trans. Robototics*, vol. 12, pp. 581 –589, aug 1996.

[8] H. Lipkin and J. Duffy, "Hybrid twist and wrench control for a robotic manipulator," *Journal of Mechanisms, Transmissions and Automation in Design*, vol. 110, pp. 138–144, 1988.

[9] A. Deal, D. L. Chow, and W. Newman, "Hybrid natural admittance control for laparoscopic surgery," in *Proc. IEEE/RSJ Int. Conf. on Intelligent Robots and Systems, Vilamoura, Algarve, Portugal*, pp. 1277–1283, 2012.

[10] W. S. Newman and Y. Zhang, "Stable interaction control and coulomb friction compensation using natural admittance control," *Journal of Robotic Systems*, vol. 11, no. 1, pp. 3–11, 1994.

[11] J. Funda, R. Taylor, B. Eldridge, S. Gomory, and K. Gruben, "Constrained cartesian motion control for teleoperated surgical robots," *Robotics and Automation, IEEE Transactions on*, vol. 12, no. 3, pp. 453–465, 1996.

[12] M. Li, A. Kapoor, and R. Taylor, "A constrained optimization approach to virtual fixtures," in *IEEE/RSJ Int. Conf. onIntelligent Robots and Systems, Alberta, Canada*, pp. 1408–1413, 2005.

[13] T. Ortmaier and G. Hirzinger, "Cartesian control issues for minimally invasive robot surgery," in *IEEE/RSJ Int. Conf. on Intelligent Robots and Systems, Takamatsu, Japan*, vol. 1, pp. 565–571 vol.1, 2000.

[14] R. Locke and R. Patel, "Optimal remote center-of-motion location for robotics-assisted minimally-invasive surgery," in *IEEE Int. Conf. on Robotics and Automation, Rome, Italy*, pp. 1900–1905, 2007.

[15] J. Lenarcic and C. Galletti, "Kinematics and modelling of a system for robotic surgery," in *On Advances in Robot Kinematics*, Springer, 2004.

[16] H. Azimian, R. Patel, and M. Naish, "On constrained manipulation in robotics-assisted minimally invasive surgery," in *IEEE RAS and EMBS Int. Conf. on Biomedical Robotics and Biomechatronics, Tokyo, Japan*, pp. 650–655, 2010.

[17] Y. Nakamura, *Advanced robotics: redundancy and optimization*. Addison-Wesley series in electrical and computer engineering: Control engineering, Addison-Wesley Longman, Incorporated, 1991.

[18] P. J. From, K. Y. Pettersen, and J. T. Gravdahl., *Vehicle-manipulator systems - modeling for simulation, analysis, and control*. London, UK: Springer Verlag, 2013.

[19] P. J. From, "On the kinematics of robotic-assisted minimally invasive surgery," *Modeling, Identification and Control*, vol. 34, no. 2, pp. 69–82, 2013.

[20] L. Sciavicco and B. Siciliano, *Modelling and Control of Robot Manipulators*. Springer, 2005.

[21] A. Blomdell, I. Dressler, K. Nilsson, and A. Robertsson, "Flexible application development and high-performance motion control based on external sensing and reconfiguration of ABB industrial robot controllers," in *Proc. IEEE Int. Conf. on Robotics and Automation, St. Paul, MN, USA*, 2010.